A Molecular Dynamics Study of the First Five Generations of Poly(Propylene Imine) Dendrimers Modified with *N*-*t*Boc-L-Phenylalanine

Luigi Cavallo* and Franca Fraternali

Abstract: A molecular dynamics study of poly(propylene imine)-based dendrimers, with end groups modified with *t*Boc-protected L-phenylalanyl amino acids, has been performed. Five generations of the dendrimer with 4, 8, 16, 32 and 64 amino acids were considered. The shape of the dendrimer was found to be generation-dependent, with higher generations more spherical. C^{α} atom radial distributions indicate that terminal amino acids are not confined to the surface, and density profiles show a hollowness for higher generations. These results suggest self-inclusion of the end groups in the inner shell and are in qualitative agreement with the experimentally proved encapsulating properties of the higher generations. Hydrogen-bond analysis indicates that a lower percentage of intraresidue hydrogen bonds occurs for higher generations. The ϕ and ψ torsional angle distributions of the amino acid end groups indicate that for higher generations an increased number of energy minima is populated. The experimentally observed decrease of the optical activity could be related to the large conformational disorder observed for higher generations.

Keywords: amino acids · computer modeling · dendrimers · molecular dynamics · stereochemistry

Introduction

One class of molecules that has received a remarkable amount of attention over the past decade are the dendrimers or starburst molecules.[1–13] Medium to large dendritic molecules are three-dimensional globular polymers with many unusual properties derived from their shape, numerous chain ends and lack of entanglements. These tree-like molecules branch out from a central core to form globular particles, and the patterns of chemical bonds in the multiple layers or generations resemble fractals. They have been hailed as promising building blocks for the fabrication of designed materials, as vehicles for controlled release of drugs,[16] as highly selective membranes[17] or as molecular scaffolds for chemical catalysts.[18] One of the major attractions of these molecules is that their size and architecture can be specifically controlled in the synthesis.[1–3, 5, 14, 15, 19] The chain ends can be opportunely functionalized in order to yield, for example, dendrimers that show different amphiphilic properties between the core and the shell, or dendrimers that can act as a support for specifically designed groups.

The poly(propylene imine) dendrimers terminated with amino acid derivatives synthesized by Meijer[20, 21] and Mühlhaupt[22] are of particular interest. These nanometric structures consist of a flexible core and a rigid chiral shell with densely packed functional groups. The core is made up of poly(propylene imine) monomers,[20] whereas the chiral shell is comprised of protected amino acid groups. Several amino acids (Ala, Leu, Phe, Tyr, Trp) generally protected by *N*-*tert*-butyloxycarbonyl (*t*Boc) groups have been used, and five generations of dendrimers with 4, 8, 16, 32 and 64 amino acids have been obtained. The fifth-generation poly(propylene imine) dendrimer is fully modified (Scheme 1),[21] whereas attempts to modify the sixth-generation poly(propylene imine) dendrimer, with 128 amino acids, have not been successful. A complete conversion has not been observed with any of the natural amino acids, probably because of severe steric hindrance.[21]

For these dendrimers an increase of the generation number results in a marked change of the molecular properties. Chiroptical studies have shown clearly that the optical activity ($[\alpha]_D$) decreases in going to higher generations, and that this phenomenon was not due to racemization, concentration, temperature or solvent effects.[21, 23] As an example, $[\alpha]_D$ in $CHCl_3$ varies from -11 to -0.1 in going from the first to the fifth generation of L-Phe-modified dendrimers. ^{13}C NMR studies have shown a significant line broadening for higher

[*] Dr. L. Cavallo
Dipartimento di Chimica, Università di Napoli
Via Mezzocannone 4,I-80134 Naples (Italy)
Fax: (+39) 81-5527771
E-mail: cavallo@chemna.dichi.unina.it
Dr. F. Fraternali
EMBL-Meyerhofstrasse 1
D-69012 Heidelberg (Germany)
E-mail: fraterna@nmr.embl-heidelberg.de
Current address: National Insitiute for Medical Research
The Ridgeway, Mill Hill, London, NW7 1AA (UK)
Fax: (+44) 181-906-4477

  0947-6539/98/0405-0927 $ 17.50+.25/0

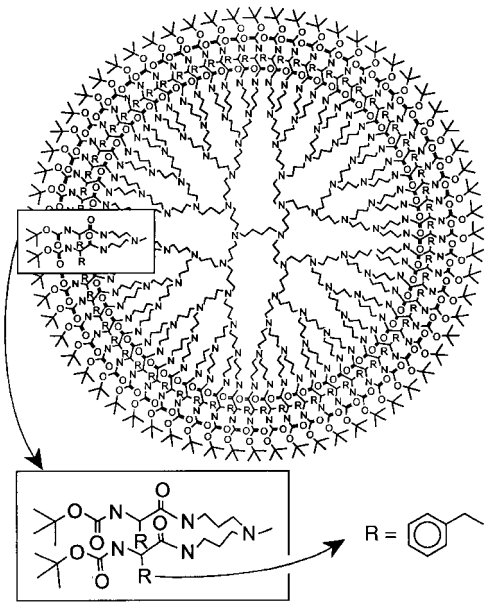

Scheme 1. The fifth-generation L-Phe-modified dendrimer.

generations,[21] indicating diminished molecular motion with an almost solid-like behaviour of the shell. This conclusion was supported by spin–lattice relaxation (T_1) measurements, which indicated higher values of T_1 for higher generations.[21]

The fifth generation of the modified dendrimer has the interesting property of encapsulating guest molecules, which gives rise to the so-called dendritic box.[21] The most ideal molecular container synthesized so far is the fifth-generation L-Phe-modified dendrimer, the 64-L-Phe box.[21] Several dyes have been encapsulated into this dendrimer by carrying out the synthesis of the 64-L-Phe box in the presence of these dyes. The guests were not released from the box even after prolonged heating and standing. Nevertheless, the liberation of the encapsulated guests can be shape-controlled.[24]

New insights into the rationalization and comprehension of the experimental behaviour of these molecules can be achieved with the help of theoretical approaches. Several authors have performed computer simulations of dendrimers. In particular, de Gennes and Hervet[25] employed a mean-field model based on the assumption that the monomers of each generation lie in a concentric shell of their own. Within this assumption they found that dendrimers can be grown up to a limiting generation, and the size of the dendrimer was proportional to $N^{0.2}$, with N being the number of monomers. The first description of dendrimers at atomic level was obtained from molecular dynamics (MD) simulations of β-alanine starburst dendrimers up to the seventh generation by Naylor et al.[26] Their analysis indicated a morphology of the dendrimers strictly dependent on the generation number, and the presence of void spaces in the interior of the dendrimers. Lescanec and Muthukumar[27] performed dendrimer simulations based on an off-lattice kinetic growth algorithm of self-avoiding walks. They found that starting from the centre of the dendrimer the density profiles decrease in a monotonic manner, and that the size of the dendrimer is proportional to $N^{0.22}$. Finally, a considerable folding of the branches was observed. Monte Carlo simulations performed by Mansfield and Klushin[28] predicted density profiles similar to those found by Lescanec and Muthukumar,[27] with the exception that the density profile for high generations shows a minimum at a certain distance from the centre. Also, they observed that the back-folding of the chains can be so extensive that monomers of higher generations can be found at any distance from the centre of the dendrimer, and that monomers belonging to different primary branches (dendrons) tend to segregate even though they are chemically identical.[29] Recently, Murat and Grest[30] performed MD simulations of model systems by varying the solvent quality. They found a strong correlation between solvent quality and mean radius of gyration, and, in contrast with previous studies,[25, 27] they observed a dendrimer size proportional to $N^{0.3\dot{3}}$. In agreement with other authors,[27, 28] considerable back-folding of the chains was found, and the amount of back-folding increased with the generation number. Segregation of the various dendrons was also detected, and the maximum dendron overlap was found for poor solvents.

These studies have helped to enlighten some of the main structure–property relationships and to ensure the applicability of standard simulation techniques to this peculiar field by studying model systems. However, at least to our knowledge, with the exception of the study of Naylor et al.,[26] there is still a lack of studies that refer to specific systems, the experimental behaviour of which is known with notable accuracy.

In this article, we investigate at atomic level the first five generations of poly(propylene imine) dendrimers modified with *N*-*t*Boc-L-phenylalanine (*n*-L-Phe dendrimers; $n = 4$, 8, 16, 32, 64) by means of MD techniques. With the aim to shed light on the experimental behaviour of these dendrimers, and in order to examine the dependence of the behaviour on the

Abstract in Italian: *In questo lavoro è riportato uno studio, effettuato con la tecnica della Dinamica Molecolare, di dendrimeri basati su poli(propilene imina), ed i cui gruppi terminali sono sostituiti con aminoacidi* L-*fenilalanina protetti da gruppi tBoc. Sono state considerate cinque generazioni di dendrimeri con 4, 8, 16, 32 e 64 gruppi aminoacidici. I dendrimeri assumono una forma tridimensionale dipendente dalla generazione, e quelli corrispondenti alle generazioni piú alte sono sostanzialmente sferici. Le distribuzioni radiali degli atomi* C^{α} *indicano che gli aminoacidi terminali non sono confinati sulla superficie del dendrimero. I profili di densitá suggeriscono la presenza di zone cave per le generazioni piú alte. Questi risultati, in accordo con le proprietá incapsulanti evidenziate da studi sperimentali, suggeriscono un'auto-inclusione dei gruppi terminali da parte dei dendrimeri. L' analisi dei ponti idrogeno mostra che i dendrimeri di generazioni piú alte formano in percentuale un numero minore di ponti idrogeno intraresiduo. Le distribuzioni degli angoli torsionali* ϕ *e* ψ *dei gruppi terminali aminoacidici, indicano che per le generazioni piú alte è popolato un numero maggiore di minimi dell' energia conformazionale. La diminuzione di attivitá ottica osservata sperimentalmente potrebbe essere correlata all' aumento di disordine conformazionale presente nelle generazioni piú alte.*

  0947-6539/98/0405-0928 $ 17.50+.50/0 *Chem. Eur. J.* **1998**, *4*, No. 5

generation number, we systematically studied the various generations up to the fifth generation. In the present study, we focus exclusively on simulations of the bare dendrimers without considering solvent effects or the behaviour in the presence of guest molecules. Solvent effects can be of relevance for low generations, whereas they should be not relevant for the more interesting fifth generation, due to the almost solid-state character of the rigid shell as demonstrated by ^{13}C NMR experiments[21] and to the fact that the peculiar chiroptical properties are not due to solvent effects.[23] Moreover, the available experimental data on these systems are in $CHCl_3$, which is a solvent with low polarity, small static dielectric constant and low ordering capacity.[31] Finally, previous studies have shown that, even for systems containing charged species, results of simulations performed in $CHCl_3$ have similar trends to those performed in vacuo.[32]

Model and Method

Description of the model: The starting structures for the simulations were built up by use of the Insight® II molecular modelling system (Biosym/MSI, San Diego).[33] The flexible cores of the five generations of the poly(propylene imine) dendrimer were built by successively adding 4, 8, 16, 32 and 64 propylene imine repeating units to the central diaminobutane unit.

The five poly(propylene imine) dendrimers were converted into the corresponding *n*-L-Phe dendrimers with a step by step growth and relaxation procedure. The following growing steps were considered: 1) building of the first peptide unit at each branch by adding alanyl residues to the NH_2 termini of the poly(propylene imine) dendrimer. The less bulky alanyl residue was chosen in order to avoid local entanglements in the first step of the building process; 2) conversion of the alanyl residues into phenylalanyl residues; 3) building of the second peptide unit at each branch by adding COOH groups to the NH_2 termini of the phenylalanyl residues; 4) conversion of the acidic COOH groups into the corresponding methyl esters $COOCH_3$; 5) conversion of the methyl group of the esters into *tert*-butyl groups. For each of these growing steps 10 ps of MD simulation at 1000 K were performed. An analogous procedure was adopted by Murat and Grest,[30] which used an equilibrated dendrimer of generation n as a core to build the dendrimer of generation $n+1$.

After the dendrimers were built, 250 ps of MD at 300 K were performed. Because with each new generation the number of end groups doubles, and in order to sample the same number of amino acids conformations, we performed 16, 8, 4, 2 and 1 MD simulations of 250 ps each, for a total of 4000, 2000, 1000, 500 and 250 ps for generations 1, 2, 3, 4 and 5, respectively, for a total of 128000 L-Phe conformations sampled for each generation. In order to check that the calculated properties of the fifth-generation dendrimer were not dependent on the length of the run, we extended the corresponding simulation to 350 ps. The average properties calculated on the last 100 ps are analogous to those obtained by analysing the conformations sampled in the 50–250 ps range. Thus, in order to analyse the same number of L-Phe conformations for all generations, in the following analysis only the conformations sampled in the 50–250 ps range were used. To further refine the different structures, the MD simulations were followed by energy minimizations.

Although the procedure followed does not ensure that the absolute minima have been obtained, we still believe that the results of the present simulations, which result from the systematic study of the different generations, can be used as tools for the rationalization of the experimental behaviour of this class of molecules.

Simulation details: The MD simulations were performed with the Discover 95.0/3.00 program (Biosym/MSI, San Diego)[34] and the different trajectories were generated by varying the random generator seed for the velocities. The temperature was kept constant by use of a direct velocity-scaling algorithm.[34] We chose to use the AMBER all-atoms force field,[35] and the cut-off radius for electrostatic interactions was set to 12.0 Å. Bonds to hydrogen atoms were kept at fixed lengths by the RATTLE algorithm.[36] The Verlet velocity algorithm,[37] as implemented in the Discover 95.0/3.00 program,[34] was used to integrate the equations of motion with a 2 fs time step. Data were collected every 0.1 ps, and the analysis was performed only on the last 200 ps of the simulation. The energy minimizations at the end of the MD runs were performed with the Discover 95.0/3.00 program.[34] The conjugate gradient algorithm was employed with a convergence criterion of 0.05 kcal mol^{-1} Å^{-1}.

Solvent-accessible surface areas and excluded volumes were computed by use of the Connolly algorithms[38, 39] as implemented in the TINKER package.[40] In these calculations hydrogen atoms were not considered. The probe radius was set to 1.4 Å. All other analyses were performed by programs developed by the authors.

Equilibration of the starting structures: Figure 1 shows the total potential energy for the different generations as a function of time. After about 50 ps all the generations were equilibrated. Average values of calculated properties and the corresponding fluctuations over the last 200 ps are given in Table 1. The energy contributions at the end of the 250 ps are given in Table 2. In order to compare energy contributions for different generations, we also report the energy contributions per atom, that is, the energy contributions are divided by the total number of atoms present in the molecule. We observed that, independent of the generation number, the energy contributions per atom have similar values, which suggests that the generated structures are reliable and also the absence of local entanglements.

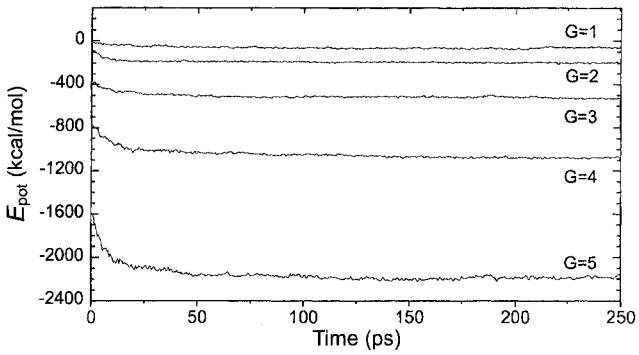

Figure 1. Time evolution of the total potential energy (E_{pot}) for the five generations (G = 1, 2, 3, 4, 5) of the dendrimer.

Results and Discussion

Dendrimer size and shape: Figure 2A shows the average radius of gyration (R_G) and the average distance of the C^α carbon atom of the Phe residues from the centre of mass of the dendrimer (R_{C^α}) as a function of the generation. The trend for the two properties is very similar. An almost linear relationship is present both for R_G and R_{C^α}. A linear fit of the type $y = a + bx$ gives values for a of 4.88 and 3.51, and for b of 2.53 and 2.89 with standard deviations of 0.41 and 0.35 Å for R_G and R_{C^α}, respectively. Figure 2B shows R_G as a function of the number of heavy atoms (N) on a log–log scale. A best fit indicates that $R_G \propto N^{0.29}$. Our result is in rough agreement with the studies of de Gennes[25] and Lescanec[27] ($R_G \propto N^{0.2}$ and $R_G \propto N^{0.22}$, respectively); however, it is in better agreement with the study of Murat[30] ($R_G \propto N^{0.33}$). It ought to be pointed out that the studies performed by de Gennes and Lescanec were based on models that did not include a thermodynamic

Table 1. Calculated average properties from the MD simulations for the five generations of *n*-L-Phe dendrimers ($n = 4, 8, 16, 32, 64$).

	4-L-Phe	8-L-Phe	16-L-Phe	32-L-Phe	64-L-Phe
R_G [Å][a]	7.7 ± 0.4	9.9 ± 0.2	12.0 ± 0.1	14.6 ± 0.1	17.8 ± 0.0
R_{C^α} dist. [Å][b]	6.3 ± 1.5	9.6 ± 2.0	11.8 ± 1.6	14.7 ± 2.6	18.2 ± 3.4
Cα fluct. [Å][c]	3.3 ± 1.7	1.8 ± 1.0	1.1 ± 0.6	1.0 ± 0.8	0.9 ± 0.7
I_x [dalton × 10^{-3} Å^{-2}][d]	25.8 ± 6.6	127.5 ± 16.4	434.9 ± 9.8	1387.2 ± 13.2	4432.7 ± 53.9
I_y [dalton × 10^{-3} Å^{-2}][d]	35.2 ± 8.6	164.7 ± 9.26	493.6 ± 10.7	1591.7 ± 14.0	4816.9 ± 22.0
I_z [dalton × 10^{-3} Å^{-2}][d]	67.3 ± 9.7	223.2 ± 13.5	619.5 ± 17.0	1948.9 ± 14.9	5802.1 ± 28.5
I_z/I_x[e]	2.6 ± 0.6	1.8 ± 0.3	1.4 ± 02	1.4 ± 0.1	1.3 ± 0.1
I_z/I_y[e]	1.9 ± 0.7	1.4 ± 0.2	1.3 ± 0.2	1.2 ± 0.1	1.2 ± 0.1
O_d[f]	0.2 ± 0.1	0.2 ± 0.1	0.1 ± 0.1	0.1 ± 0.0	0.1 ± 0.0
E_{pot} [kcal mol^{-1}][g]	− 53.4 ± 8.1	− 189.1 ± 12.1	− 514.2 ± 7.4	− 1062.9 ± 16.1	− 2142.8 ± 33.8

[a] R_G is the radius of gyration. [b] R_{C^α} dist. is the distance of the C$^\alpha$ atom of the Phe residues from the centre of mass of the dendrimer. [c] C$^\alpha$ fluct. is the fluctuation of the C$^\alpha$ atom of the Phe residues. [d] I_x, I_y and I_z are the moments of inertia along the principal axes sorted in ascending order. [e] I_z/I_x and I_z/I_y are the ratio of the moments of inertia I_z and I_x, and I_z and I_y. [f] O_d is the total overlap of the four dendrons (see text). [g] E_{pot} is the total potential energy.

Table 2. Energy contributions and energy contributions per atom for the five generations of *n*-L-Phe dendrimers ($n = 4, 8, 16, 32, 64$) after energy minimization at the end of 250 ps of MD at 300 K.

	4-L-Phe	8-L-Phe	16-L-Phe	32-L-Phe	64-L-Phe
	Energy [kcal mol^{-1}]				
total	− 182.8	− 473.7	− 1081.6	− 2198.7	− 4446.1
internal	41.9	97.7	289.3	610.6	1256.1
nonbonded	− 224.7	− 571.4	− 1370.9	− 2809.3	− 5702.2
	Energy per atom [kcal mol^{-1}][a]				
total	− 0.92	− 1.11	− 1.22	− 1.23	− 1.23
internal	0.21	0.23	0.33	0.34	0.35
nonbonded	− 1.13	− 1.34	− 1.55	− 1.57	− 1.58

[a] For the energy contributions per atom, the various terms in the upper part of the table are divided by the total number of atoms present in the molecule.

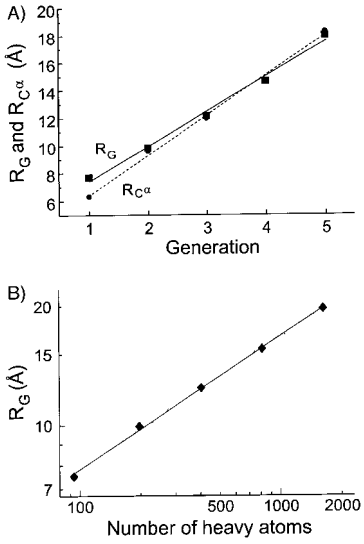

Figure 2. A) Average radius of gyration (R_G; continuous line) and average distance of the C$^\alpha$ atom of the Phe residues (R_{C^α}; dashed line) as a function of the generation. B) R_G as a function of the number of heavy atoms of the dendrimer, on a log–log scale.

relaxation of the generated structures, whereas the simulations performed by Murat included such an equilibration before data collection.

Figure 3 displays plots of the ratios of the average moments of inertia along the principal axes x, y and z. We have assumed

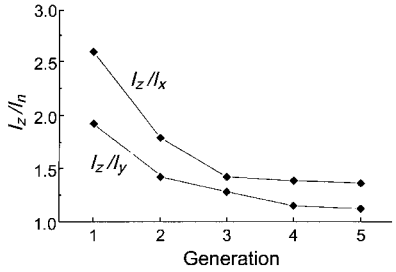

Figure 3. Relative values I_z/I_x and I_z/I_y of the three principal moments of inertia ($I_x < I_y < I_z$) as a function of the generation.

that $I_x < I_y < I_z$, and we have plotted the ratios I_z/I_x and I_z/I_y. Low-generation dendrimers are highly asymmetric, indicated by the high values of the I_z/I_x and I_z/I_y. At higher generations these ratios approach unity, indicating that the dendrimers are becoming progressively more spherical. These results are in agreement with findings of others authors.[26, 28]

C$^\alpha$-atom radial distributions and fluctuations: Figure 4 shows the radial distributions of the C$^\alpha$ carbon atom of the Phe residues (calculatated as the fraction of C$^\alpha$ atoms per unit volume) as a function of the distance from the centre of mass of the dendrimer. For low-generation dendrimers the curves are symmetrical and have narrow distributions. This suggests that all the L-Phe residues are on the surface of the molecule. On the other hand, for high-generation dendrimers the curves are not symmetrical and have long tails, indicating that a significant back-folding of the end groups occurs, and that monomers of the last generations penetrate the interior of the molecule almost to the core. This result is in agreement with previous observations on model systems.[27, 28, 30] In conclusion, considering the encapsulating properties of the fifth-generation dendrimer a back-folding of the chains is reasonable and can be thought of as a self-encapsulation of the bulky end groups. The driving force could be a natural tendency to relax the steric hindrance at the surface of higher generations.

The average C$^\alpha$-atom fluctuations reported in Table 1 clearly indicate a diminished flexibility for higher generations. This result suggests a closer packing of the dendrimers of the higher generations and is in good qualitative agreement with the rigidity demonstrated by ^{13}C NMR relaxation measurements.[21]

0947-6539/98/0405-0930 $ 17.50+.50/0 *Chem. Eur. J.* **1998**, *4*, No. 5

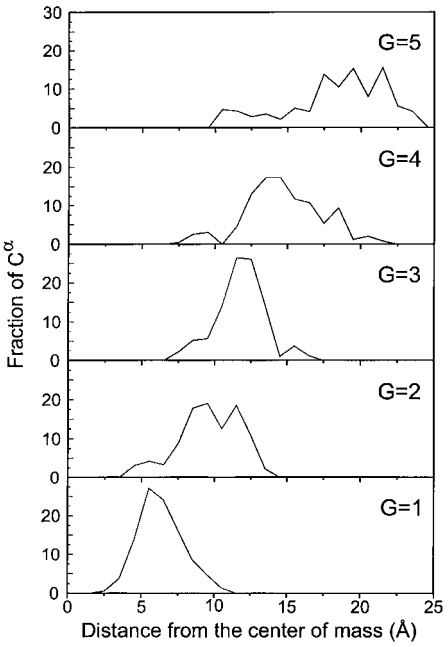

Figure 4. Radial distributions of the C^{α} atom of the Phe residues as a function of the distance from the centre of mass of the dendrimer for the five generations (G = 1, 2, 3, 4, 5).

Density profiles: Figure 5 shows plots of the average atom densities (number of atoms per unit volume) as a function of the distance from the centre of mass of the dendrimer. A

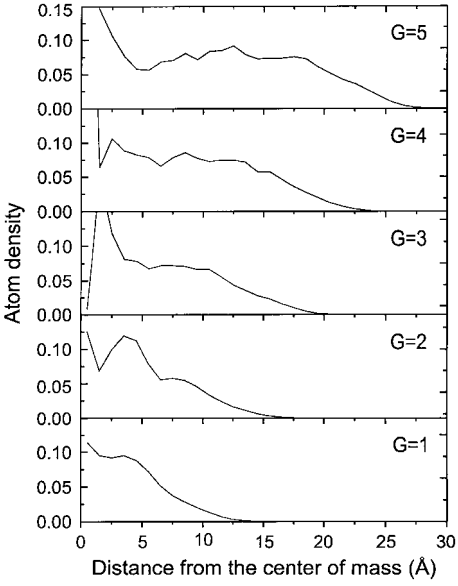

Figure 5. Radial atom densities as a function of the distance from the centre of mass of the dendrimer for the five generations (G = 1, 2, 3, 4, 5).

common feature is a region of high density near the centre of the molecule. As observed by other authors,[28, 30] density profiles corresponding to lower generations decrease almost monotonically, while for higher generations a well-defined minimum, and hence a low-density region, is present.[28, 30] A region of low density in the interior of the fifth-generation dendrimer, even in the presence of back-folding of the bulky end groups, is in qualitative agreement with the encapsulating properties of the 64-L-Phe box.

Dendron segregations: The segregation of the dendrons was evaluated according to the procedure described by Murat and Grest.[30] The space occupied by the dendrimers is divided into cubic cells, and the number of atoms belonging to dendron x that are inside the cell is defined as $\psi_x(i,j,k)$, with the indices i, j and k used to identify the cells. The total overlap O_d is defined in Equation (1).

$$O_d = \frac{\sum^{(i,j,k)} \psi_1\psi_2 + \psi_1\psi_3 + \psi_1\psi_4 + \psi_2\psi_3 + \psi_2\psi_4 + \psi_3\psi_4}{\sum^{(i,j,k)} \psi_1^2 + \psi_2^2 + \psi_3^2 + \psi_4^2} \quad (1)$$

The sum is over all the cells, and ψ_x is equal to $\psi_x(i,j,k)$. If the dendrons are completely segregated, for each cell only one value of $\psi_x(i,j,k)$ is not zero, and the total overlap O_d is equal to zero. On the other hand, if the dendrons are totally mixed for each cell the $\psi_x(i,j,k)$ values are equal to each other, and the total overlap (O_d) is equal to 1.5. The particular value assumed by O_d depends on the size of the cell. In the following analysis we chose a cell length of 5.0 Å. Although for different values of the cell length the absolute numeric values of O_d are different, no reasonable adjustment of the cell length can modify the conclusions of this analysis.

Figure 6 shows plots of O_d as a function of the generation. In agreement with the results of other authors,[29, 30] a noticeable segregation of the dendrons is observed. As found by Murat and Grest,[30] the amount of overlap decreases with increasing generation number.

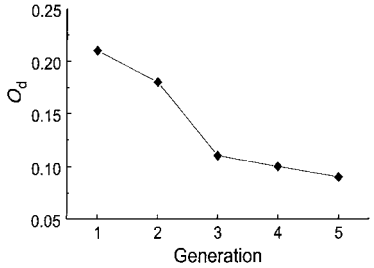

Figure 6. Total overlap (O_d) of the various dendrons as a function of the generation.

Hydrogen-bond patterns: The average percentage of H-bonds observed in the performed simulations are reported in Table 3. For each Phe residue two donor nitrogen atoms are present. Thus, 8, 16, 32, 64 and 128 donors are present for generations 1 to 5, respectively. These numbers coincide with the maximum number of H-bonds (HB_{max}) on the assumption that each donor participates in one H-bond only. H-bond acceptors are represented by the three oxygen atoms of each Phe residue (two from the amide groups and one in the ester *t*Boc unit) and by all the sp^3 nitrogen atoms of the propylimine spacers. According to this we have 14, 30, 62, 126 and 254 acceptors for generations 1 to 5, respectively.

The observed H-bonds are reported as those formed by a donor and an acceptor that belong to the same residue (C_5, C_7 and PC_7 types) or to different residues (external H-bonds, Ex_O

Table 3. Calculated average percentages of H-bonds from the MD simulations for the five generations of *n*-L-Phe dendrimers ($n = 4$, 8, 16, 32, 64).

H-bond	4-L-Phe	8-L-Phe	16-L-Phe	32-L-Phe	64-L-Phe
C_5[a]	1.2	0.4	0.1	2.4	0.7
C_7[a]	39.5	45.1	35.4	35.8	18.0
PC_7[b]	0.0	0.0	2.9	0.7	4.8
Ex_O[c]	6.2	5.3	3.7	8.7	14.7
Ex_N[c]	0.4	0.1	0.1	0.3	0.3
intra residue[d]	40.7	45.5	38.4	38.9	23.5
inter residue[d]	6.6	5.4	3.8	9.0	15.0
total	47.3	50.9	42.2	47.9	38.5

[a] C_5 and C_7 represent H-bonds that determine 5- and 7-membered rings in the same Phe residue. [b] PC_7 is a pseudo C_7 conformation in which the seven-membered ring is determined by an H-bond interaction of the first amidic nitrogen of the Phe residue and the oxygen of the ester *t*Boc. [c] Ex_O and Ex_N are H-bonds with oxygens of different Phe residues or sp^3 nitrogens of the propylimine spacers, respectively. [d] The intra- and interresidue percentages are the sum of the C_5, C_7, PC_7 and Ex_O, Ex_N percentages, respectively.

and Ex_N types) of the dendrimer. C_5 and C_7 represent typical conformations observed in peptide systems,[41] with H-bonds completing a 5- or 7-membered ring within the same Phe residue. PC_7 is a pseudo C_7 conformation in which the seven-membered ring is determined by an H-bond interaction between the first amide nitrogen of the Phe residue and the oxygen of the ester *t*Boc group. Ex_O and Ex_N are H-bonds to oxygen atoms of different Phe residues or to sp^3 nitrogens of the propylimine spacers, respectively. An H-bond is considered to occur if the distance between the hydrogen atom and the acceptor is smaller than 2.5 Å and the angle donor-H-acceptor is greater than 90°. The percentage of H-bonds is calculated according to the formula $\%HB = 100 \times HB_{obs}/HB_{max}$, where HB_{obs} represents the number of H-bonds observed in the sampled frame (defined previously).

The total percentage of H-bonds decreases markedly in the fifth generation, which suggests an increased disorder in the corresponding structure. The percentage of C_7 H-bonding is almost halved, while a noticeable increase of the percentage of Ex_O H-bonds is observed. As a consequence, the amount of intraresidue H-bonds considerably decreases with a concerted increase of interresidue H-bonds. As a hypothesis, the augmented steric hindrance in the molecule prevents the dendrimer branches from adopting folded intraresidue structures and forces the interresidue interactions to occur. As suggested by Meijer, a higher percentage of interresidue H-bonds could contribute to the experimentally observed rigidity of the fifth-generation dendrimer. This conclusion is also consistent with the reduced C^α-atom fluctuations previously discussed. Finally, a negligible amount of H-bonding to the nitrogen atoms of the propylimine spacers occurs, probably due to the high steric hindrance in the proximity of these triply substituted atoms.

ϕ and ψ torsional angle distributions: The Ramachandran plot[41] of the peptide acetyl-L-Phe-*t*Boc is shown in Figure 7A. The lowest energy minimum is found for the symmmetric C_{7eq} $(\phi, \psi) \equiv (-60°, 60°)$ conformation[41] with its symmetric one, C_{7ax} $(60°, -60°)$,[41] close in energy. The other detected minima

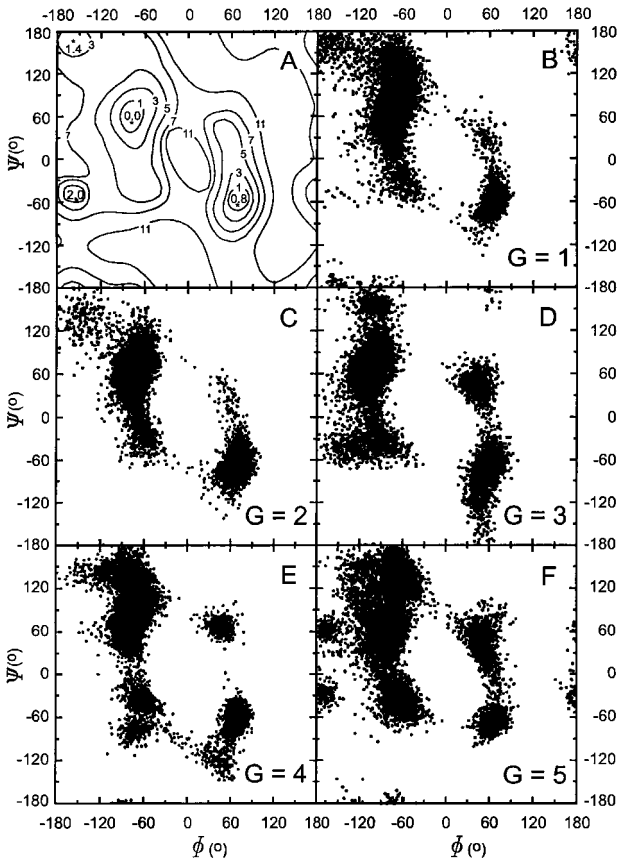

Figure 7. A) Ramachandran plot of the peptide Acetyl-L-Phe-*t*Boc (the isoenergetic curves are drawn at 1, 3, 5, 7, and 11 kcal mol^{-1}). B)–F) The calculated ϕ and ψ torsional angle distributions of the Phe residues, for the five generations (G = 1, 2, 3, 4, 5).

are in the C_5 (180°,180°),[41] α' (180°, −60°)[42] and P_{II} (−60°,180°)[42] regions.

The calculated values of the ϕ and ψ torsional angles[41] of the Phe residues during the MD simulations for the first- to fifth-generation dendrimers are shown in Figures 7B–7F, respectively. For each generation, the same number of points has been collected (see methods). Independent of the generation number, the most populated energy minimum corresponds to the C_{7eq} conformation. Nevertheless, for higher generations more minima are populated. In particular, for the fifth generation an increased number of minima is observed with a wider spread of the allowed conformations. A larger percentage of α helix conformers of both helicities is present, and the α' and P_{II} semiextended structures are more populated. These structures are not intrinsically stabilized by H-bonds in a dipeptide and are usually stable for longer peptide chains. In this case, increasing the generation number corresponds to an augmented proximity of the amino acid residues, and this induces the folding in these conformations. This is in agreement with the previously discussed H-bonds analysis in which the reduced flexibility, due to the greater steric hindrance in higher generations, leads to a greater number of interresidue H-bonds to the detriment of conformations with intraresidue H-bonds.

The higher conformational disorder of the Phe residues could rationalize the vanishing optical activity of the higher

0947-6539/98/0405-0932 $ 17.50+.50/0 *Chem. Eur. J.* **1998**, *4*, No. 5

generations, as already suggested by Meijer et al.[23] If the molecular environment forces the amino acid residues into different energy minima, an internal compensation effect of different chiral conformers could cause the decrease of the optical activity of the higher generations.[43]

Table 4. Calculated average solvent-accessible surface areas (SASA) and excluded volumes (EV) from the MD simulations for the five generations of *n*-L-Phe dendrimers ($n = 4, 8, 16, 32, 64$).

	4-L-Phe	8-L-Phe	16-L-Phe	32-L-Phe	64-L-Phe
$SASA_{apol}$ [Å^2][a]	1432.8	2690.0	5061.7	8215.3	13280.5
$SASA_{pol}$ [Å^2][a]	180.3	342.7	678.8	946.9	1434.9
$SASA_{tot}$ [Å^2][a]	1613.1	3032.7	5740.5	9162.2	14715.4
EV_{tot} [Å^3][a]	3366.0	6915.6	13976.2	26632.4	50777.5
			Values per atom[b]		
$SASA_{tot}$ [Å^2]	17.3	15.4	14.2	11.2	8.9
EV_{tot} [Å^3]	36.2	35.1	34.5	32.4	30.7

[a] $SASA_{apol}$, $SASA_{pol}$, $SASA_{tot}$ and EV_{tot} represent the apolar, polar and total solvent-accessible surface areas, and total excluded volume, respectively. [b] The per atom contributions have been obtained by dividing the total values by the total number of non-hydrogen atoms.

Solvent-accessible surface areas and excluded volumes: The average solvent-accessible surface area[38] and excluded volume[39] observed in the performed simulations are given in Table 4. For the sake of comparison the per atom contributions are also reported. In this case, the total average areas and volumes are divided by the total number of heavy atoms present in the molecule.

The augmented proximity of the various residues in higher generations, already suggested by the H-bond, and ϕ and ψ torsional angle analyses, is confirmed. On increasing the generation number, an almost linear decrease of the solvent-accessible surface area and excluded volume per atom is observed. In particular, the solvent-accessible surface area per atom is almost halved in going from the first to the fifth generation. This analysis is consistent with a more dense packing of the residues for higher generations.

The apolar contribution to the solvent-accessible surface area is close to 90% and is independent of the generation. Considering that the percentage of apolar atoms in the dendrimers is close to 75%, this indicates that polar atoms are shielded by the hydrophobic moiety of the dendrimer.

Conclusions

We have presented a molecular dynamics investigation on the first five generations of poly(propylene imine) dendrimers modified with *N*-*t*Boc-L-phenylalanine amino acid end groups. The main results of the present study are the following: i) The dendrimer size is found to follow the relationship $R_G \propto N^{0.29}$, with R_G and N being the radius of gyration and the number of heavy atoms, respectively. ii) The diminished fluctuation of the C^α atoms of the amino acid residues for higher generations suggests a denser packing and a greater rigidity for these molecules. This result is in qualitative agreement with the experimental finding of a high-density solid-like packing in solution demonstrated by ^{13}C NMR relaxation measurements.[21] iii) The radial distribution of the C^α atoms clearly indicate that for higher generations a noticeable back-folding of the end groups occurs. Moreover, for the higher generations some hollowness is indicated by the radial atom density analysis. Consequently, even if self-encapsulation of the bulky termini occurs, it is not able to completely fill the voids created between the propylimine spacers. This self-encapsulation property is clearly coherent with the experimentally proved encapsulating properties of the 64-L-Phe box. iv) H-bond analysis indicates a decrease of the intraresidue H-bonds for the higher generations and, as a consequence, for higher generations a higher number of less ordered structures is present. v) The ϕ and ψ torsional angle distribution analysis indicates that for higher generations a larger number of minima in the Ramachandran plot are populated. These conformations are probably enforced by the denser packing, as seen by the smaller per atom solvent-accessible surface area and excluded volume obtained for higher generations. These results support the hypothesis of Meijer et al. that the vanishing optical activity of higher generations could be ascribed to presence of a higher conformational disorder of the amino acid residues.[23]

More complete experimental data on these systems are highly desirable. The field is rapidly developing and more detailed structural and thermodynamic characterizations are more than welcome. Modelling work, although never equivalent to any experimental proof, we hope contributes towards gaining an insight on new systems and to stimulate new experiments. The reasonable qualitative agreement with the available experimental results of the present simulations is also encouraging for the application of MD simulation techniques to this class of molecules.

Note added in proof: Shortly after this manuscript was submitted, the following two papers were published: P. Miklis, T. Cagin, W. A. Goddard III *J. Am. Chem. Soc.*, **1997**, *119*, 7458 and H. W. I. Peerlings, E. W. Meijer *Chem. Eur. J.*, **1997**, *3*, 1563. In the first paper, molecular dynamics simulations have been performed on the fifth-generation dendrimer with 4 to 6 bengal rose molecules and also with explicit solvent molecules. The gyration radius they calculated ($\approx$19 Å) is in good agreement with our value of $\approx$18 Å for the same generation dendrimer, especially considering that we performed our simulations in absence of any guest molecules. In the second paper, the issue of dense packing at the surface has been investigated by introduction of an alkyl chain spacer between the *t*Boc-L-Phe amino acids and the end of the branching of the poly(propylene imine) core. The dendrimers of the first and fifth generation were synthesized and compared with the chiral dendrimer without spacers. The optical activity remains constant for both derivatives with spacers, which is in contrast to the decrease in optical activity for the dendrimers without. The authors suggest that with the spacer the L-Phe units can freely adopt the preferred conformation, whereas without the spacers the L-Phe units are forced to adopt different frozen-in conformations. Our results (conformational disorder for the fifth generation

without spacers) is in good qualitative agreement with these very elegant experiments.

Acknowledgments: We thank the Istituto Guido Donegani S.p.A. (ENICHEM) for the opportunity to use the Biosym/MSI software. The financial support of the M.U.R.S.T. is gratefully acknowledged.

Received: July 21, 1997 [F774]

[1] E. Buhleier, W. Wehner, F. Vögtle, Synthesis **1978**, 155.
[2] G. R. Newkome, Z. Q. Yao, G. R. Baker, V. K. Gupta, *J. Org. Chem.* **1985**, *50*, 2003.
[3] D. A. Tomalia, H. Baker, J. R. Dewald, M. J. Hall, G. Kallos, S. J. Martin, J. Roeck, J. Ryder, P. B. Smith, *Polym. J.* **1985**, *17*, 117.
[4] D. A. Tomalia, J. R. Dewald, M. J. Hall, S. J. Martin, P. B. Smith, *Macromolecules* **1986**, *19*, 2466.
[5] C. Hawker, J. M. J. Fréchet, *J. Chem. Soc. Chem. Commun.* **1990**, 1010.
[6] D. A. Tomalia, A. M. Naylor, W. A. Goddard III, *Angew. Chem.* **1990**, *102*, 119; *Angew. Chem. Int. Ed. Engl.* **1990**, *29*, 138.
[7] G. R. Newkome, X. Lin, *Macromolecules* **1991**, *24*, 1443.
[8] D. A. Tomalia, H. D. Durst, *Top. Curr. Chem.* **1993**, *165*, 193.
[9] G. H. Escamilla, G. R. Newkome, *Angew. Chem.* **1994**, *106*, 2013; *Angew. Chem. Int. Ed. Engl.* **1994**, *33*, 1937.
[10] J. C. M. van Hest, D. A. P. Delnoye, M. W. P. Baars, M. H. P. van Genderen, E. W. Meijer, *Science* **1995**, *268*, 1592.
[11] J. M. J. Fréchet, M. Henmi, I. Gitsov, S. Aoshima, M. R. Leduc, R. B. Grubbs, *Science* **1995**, *269*, 1080.
[12] S. C. Zimmerman, F. Zeng, D. E. C. Reichert, S. V. Kolotuvhin, *Science* **1996**, *271*, 1095.
[13] T. W. Bell, *Science* **1996**, *271*, 1077.
[14] G. R. Newkome, C. N. Moorefield, in *Comprehensive Supramolecular Chemistry, Vol. 10* (Ed.: D. N. Reinhoudt), Elsevier, New York, **1996**, chapter 26.
[15] G. R. Newkome, C. N. Moorefield, F. Vögtle, *Dendritic Molecules: Concepts, Syntheses and Perspectives*, VCH, Weinheim (Germany), **1996**.
[16] J. C. Roberts, Y. E. Adams, D. A. Tomalia, J. A. Mercer-Smith, D. K. Lavallee, *Bioconjugate Chem.* **1990**, *2*, 305.
[17] K. R. Godpias, A. R. Leheny, G. Camianati, N. J. Turro, D. A. Tomalia, *J. Am. Chem. Soc.* **1991**, *113*, 7335.
[18] J. W. J. van Knapen, A. W. van der Made, J. C. de Wilde, P. W. N. M. van Leeuwen, P. Wijkens, D. M. Grove, G. van Koten, *Nature* **1994**, *372*, 659.
[19] C. J. Hawker, J. M. J. Fréchet, *J. Am. Chem. Soc.* **1990**, *112*, 7638.
[20] E. M. M. de Brabander-van den Berg, E. W. Meijer, *Angew. Chem.* **1993**, *105*, 1370; *Angew. Chem. Int. Ed. Engl.* **1993**, *32*, 1308.
[21] J. F. G. A. Jansen, E. M. M. de Brabander-van den Berg, E. W. Meijer, *Science* **1994**, *266*, 1226.
[22] C. Wörner, R. Mühlhaupt, *Angew. Chem.* **1993**, *105*, 1367; *Angew. Chem. Int. Ed. Engl.* **1993**, *32*, 1306.
[23] J. F. G. A. Jansen, H. W. I. Peerlings, E. M. M. de Brabander-van den Berg, E. W. Meijer, *Angew. Chem.* **1995**, *107*, 1321; *Angew. Chem. Int. Ed. Engl.* **1995**, *34*, 1206.
[24] J. F. G. A. Jansen, E. W. Meijer, E. M. M. de Brabander-van den Berg, *J. Am. Chem. Soc.* **1995**, *117*, 4417.
[25] P. G. de Gennes, H. Hervet, *J. Phys. Lett. Fr.* **1983**, *44*, L351.
[26] A. M. Naylor, W. A. Goddard III, G. E. Kiefer, D. A. Tomalia, *J. Am. Chem. Soc.* **1989**, *111*, 2339.
[27] R. L. Lescanec, M. Muthukumar, *Macromolecules* **1990**, *23*, 2280.
[28] M. Mansfield, L. Klushin, *Macromolecules* **1993**, *26*, 4262.
[29] M. Mansfield, *Polymer* **1994**, *35*, 1827.
[30] M. Murat, G. S. Grest, *Macromolecules* **1996**, *29*, 1278.
[31] I. G. Tironi, W. F. van Gunsteren, *Mol. Phys.* **1994**, *83*, 381.
[32] M. Lauterbach, G. Wipff, *Supramol. Chem.* **1995**, *6*, 187.
[33] Insight® II User Guide, Biosym/MSI, San Diego, **1995**.
[34] Discover® 95.0/3.00 User Guide, Biosym/MSI, San Diego, **1995**.
[35] S. J. Weiner, P. A. Kollman, D. A. Case, U. C. Singh, C. Ghio, G. Alagona, S. Profeta, Jr., P. Weiner, *J. Am. Chem. Soc.* **1984**, *106*, 765.
[36] H. C. Andersen, *J. Comp. Phys.* **1983**, *52*, 24.
[37] L. Verlet, *Phys. Rev.* **1967**, *159*, 98.
[38] M. L. Connolly, *J. Appl. Cryst.* **1983**, *16*, 548.
[39] M. L. Connolly, *J. Am. Chem. Soc.* **1985**, *107*, 1118.
[40] M. Dudek, J. Ponder, *J. Comput. Chem.* **1995**, *16*, 791.
[41] C. R. Cantor, P. R. Schimmel, *Biophysical Chemistry Vol. 1* (Ed.: W. H. Freemer), San Francisco, **1980**.
[42] E. Bendetti, in *Chemistry and Biochemistry of Aminoacids, Peptides and Proteins* (Ed.: B. Weinstein), Marcel Dekker, New York, **1982**, p. 105.
[43] M. M. Green, B. A. Garetz, *Tetrahedron Lett.* **1984**, *25*, 2831.